

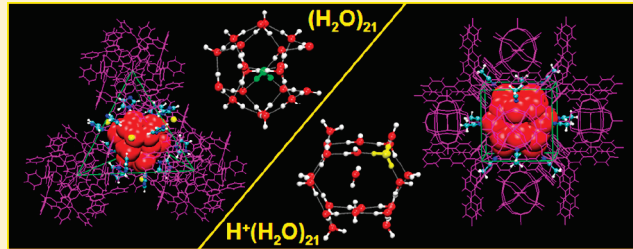
# Structures of Neutral and Protonated Water Clusters Confined in Predesigned Hosts: A Quantum Mechanical/Molecular Mechanical Study

Zhen Yang, Shugui Hua, Weijie Hua, and Shuhua Li\*

School of Chemistry and Chemical Engineering, Key Laboratory of Mesoscopic Chemistry of the Ministry of Education, Institute of Theoretical and Computational Chemistry, Nanjing University, Nanjing 210093, People's Republic of China

 Supporting Information

**ABSTRACT:** Hybrid quantum mechanical/molecular mechanical (QM/MM) calculations have been carried out to investigate the structures of the neutral  $(\text{H}_2\text{O})_{21}$  and protonated  $\text{H}^+(\text{H}_2\text{O})_{21}$  clusters confined in the crystal hosts. The influence of other cocrystallized species and the local electrostatic environments of the crystal hosts on the structures of water clusters has been analyzed. For the neutral  $(\text{H}_2\text{O})_{21}$  cluster in the tetrahedral host, its low-lying structures are found to exist as a dodecahedral cage with one interior water molecule, which is in good accord with the corresponding X-ray data. The confined  $(\text{H}_2\text{O})_{21}$  cluster possesses the main structural features of the lowest-energy structure of the free  $(\text{H}_2\text{O})_{21}$  cluster in the gas phase. For the protonated  $\text{H}^+(\text{H}_2\text{O})_{21}$  cluster confined in the cubic cavity, its low-lying structures are found to have a common hexahedral  $(\text{H}_2\text{O})_{20}$  shell, which is consistent with the experimental X-ray structure, but the position of the additional  $\text{H}_2\text{O}$  (or the  $\text{H}_3\text{O}^+$  ion) in different low-lying structures is different, while the  $\text{H}_3\text{O}^+$  ion is situated at the center of the cage in the corresponding X-ray structure. The overall shape of the confined  $\text{H}^+(\text{H}_2\text{O})_{21}$  cluster is significantly different from that of the free cluster in the gas phase, and the confined cluster has much less intrinsic hydrogen bonds (H-bonds) than the free cluster, due to the need to form extrinsic H-bonds with acetonitrile molecules in the crystal host. The local electrostatic environment of the crystal host is found to exert a negligible influence on the structure of the  $(\text{H}_2\text{O})_{21}$  cluster but play a significant role in modulating the structure of the  $\text{H}^+(\text{H}_2\text{O})_{21}$  cluster. This may be attributed to the fact that the protonated water cluster is much more easily polarized by the external electrostatic field of the crystal host than the neutral water cluster.



## 1. INTRODUCTION

Water clusters have attracted considerable attention because of their fundamental importance in chemical and biological processes.<sup>1–5</sup> Experimental and theoretical studies on neutral and protonated water clusters have greatly deepened our understanding of the hydrogen-bond (H-bond) networks and proton transfer in water.<sup>6–8</sup> Compared to small clusters, the detailed structural information of large water clusters ( $n > 20$ ) is still scarce, since spectroscopic characterization of gas-phase large water clusters is difficult because of the presence of many low-lying isomers under experimental conditions.<sup>9</sup> Recently, the experimental scientists have developed an efficient approach to explore the structures of water clusters. They successfully trapped various neutral<sup>10–16</sup> and protonated<sup>17,18</sup> water clusters inside predesigned crystal hosts, such as organic materials and metal–organic frameworks (MOFs). The lattice of a predesigned crystal host can provide a confining environment to stabilize these water clusters, and then the relevant crystallographic characterization could offer the detailed structural information, which cannot be directly obtained with other experimental methods.

With this strategy, the structures of several large water clusters,  $(\text{H}_2\text{O})_n$  and  $\text{H}^+(\text{H}_2\text{O})_n$  ( $n > 20$ ) have been characterized in

recent years.<sup>16–18</sup> For example, Ye et al.<sup>16</sup> reported the structure of a  $(\text{H}_2\text{O})_{21}$  cluster, which was embedded in a tetrahedral host constructed by four ionic clusters  $[\text{Co}(\text{H}_2\text{O})_6\subset\text{Co}_8\text{L}_{12}]^{6+}$  [ $\text{HL} = 4,6\text{-di(2-pyridyl)-1,3,5-triazine-2-ol}$ ]. The X-ray structural analysis revealed that this cluster exists as a pentagonal dodecahedral cage with one water molecule inside the cage. This structural feature of the  $(\text{H}_2\text{O})_{21}$  cluster seems to be in good agreement with the previous theoretical studies.<sup>19–22</sup> On the other hand, Duan et al.<sup>17</sup> showed that the protonated water cluster,  $\text{H}^+(\text{H}_2\text{O})_{21}$ , can be captured in the cubic cavity provided by the porous MOFs,  $\{[\text{Co}_4(\text{dpdo})_{12}][\text{H}(\text{H}_2\text{O})_{21}(\text{CH}_3\text{CN})_{12}][\text{PM}_{12}\text{O}_{40}]_3\}_\infty$  ( $\text{dpdo} = 4,4'\text{-bipyridine-}N,N'\text{-dioxide}, \text{M} = \text{Mo, W}$ ). The cluster,  $\text{H}^+(\text{H}_2\text{O})_{21}$ , is structurally characterized as a hexahedral  $(\text{H}_2\text{O})_{20}$  shell with a  $\text{H}_3\text{O}^+$  ion in the cage. The structural feature revealed by this study is considerably different from the model proposed by Searcy and Fenn.<sup>23</sup> They suggested that  $\text{H}^+(\text{H}_2\text{O})_{21}$  in the gas phase might exist as a pentagonal dodecahedron with one neutral water molecule in the cage and a  $\text{H}_3\text{O}^+$  ion on the

**Received:** April 2, 2011

**Revised:** June 2, 2011

**Published:** June 02, 2011

surface, which has been verified to be a low-energy structure by many theoretical calculations.<sup>24–28</sup>

It should be noted that water clusters trapped in the crystal hosts are often stabilized by extrinsic H-bond interactions between other small organic molecules or ions (in the hosts) and water molecules. For example, in the crystal host designed by Ye et al.,<sup>16</sup> the  $(\text{H}_2\text{O})_{21}$  cluster is hydrogen-bonded to 12 imidazole molecules and 4  $\text{Br}^-$  ions. In the host designed by Duan et al.,<sup>17</sup> the  $\text{H}^+(\text{H}_2\text{O})_{21}$  cluster is stabilized by the extrinsic H-bonds with 12 acetonitrile molecules. Thus, one can expect that the structures of neutral or protonated water clusters in the crystal hosts result from the competition between intrinsic H-bonds (of water clusters) and extrinsic H-bonds (between water clusters and other molecules or ions). On the other hand, the confinement of the hosts and the local electrostatic environments of the crystal hosts is also supposed to play some role in tuning the structures of various water clusters. Therefore, it is very desirable to theoretically investigate how the factors mentioned above influence the structures of various water clusters confined in the crystal hosts. In addition, it is well-known that the crystallographic characterization could not directly locate the position of the hydrogen atoms in water clusters. Thus, the detailed information on the possible H-bond network and the nature of the proton (the Eigen form:  $\text{H}_3\text{O}^+$  or the Zundel form:  $\text{H}_5\text{O}_2^+$ ) in the neutral and protonated water clusters cannot be determined according to the experimental X-ray data. However, such information can be directly obtained with theoretical computations at a molecular level.

In this work, we will employ a hybrid quantum mechanical/molecular mechanical (QM/MM) method to investigate the structural features of two large water clusters,  $(\text{H}_2\text{O})_{21}$  and  $\text{H}^+(\text{H}_2\text{O})_{21}$ , confined in the crystal hosts as described above.<sup>16,17</sup> Among various water clusters, the 21-molecule clusters represent the “magic number” structures,<sup>29,30</sup> because they show enhanced stability compared to the neighboring clusters. By comparing the low-lying structures of  $(\text{H}_2\text{O})_{21}$  and  $\text{H}^+(\text{H}_2\text{O})_{21}$  clusters confined in the crystal hosts with those in vacuum, we have analyzed the influence of surroundings on the cluster structures. Additionally for the  $\text{H}^+(\text{H}_2\text{O})_{21}$  case, the position and nature of the proton in the confined cluster are also investigated. These calculations are of great help for experimental scientists to better design and synthesize the new crystal hosts for encapsulating more water clusters.

## 2. COMPUTATIONAL METHODS

**2.1. Hybrid QM/MM Method.** To study the neutral and protonated water clusters confined in the crystal hosts, we have constructed two different model systems according to the experimental work by Ye et al. and Duan et al., respectively.<sup>16,17</sup> As shown in Figure 1, we partition it into a QM region (the ball and stick style) and a MM region (the wireframe style), since each model system is too big for full QM calculations. For convenience, the model systems of the  $(\text{H}_2\text{O})_{21}$  and  $\text{H}^+(\text{H}_2\text{O})_{21}$  clusters are denoted as Model 1 and Model 2, respectively. In Model 1, the QM region consists of the  $(\text{H}_2\text{O})_{21}$  cluster, 12 imidazole molecules, and four  $\text{Br}^-$  ions, while the MM region consists of four  $[\text{Co}(\text{H}_2\text{O})_6 \subset \text{Co}_8\text{L}_{12}]^{6+}$  clusters. For Model 2, the QM region consists of the  $\text{H}^+(\text{H}_2\text{O})_{21}$  cluster and 12 acetonitrile molecules, while the MM region includes the partial MOF  $[\text{Co}_8(\text{dpdo})_{36}]$  and

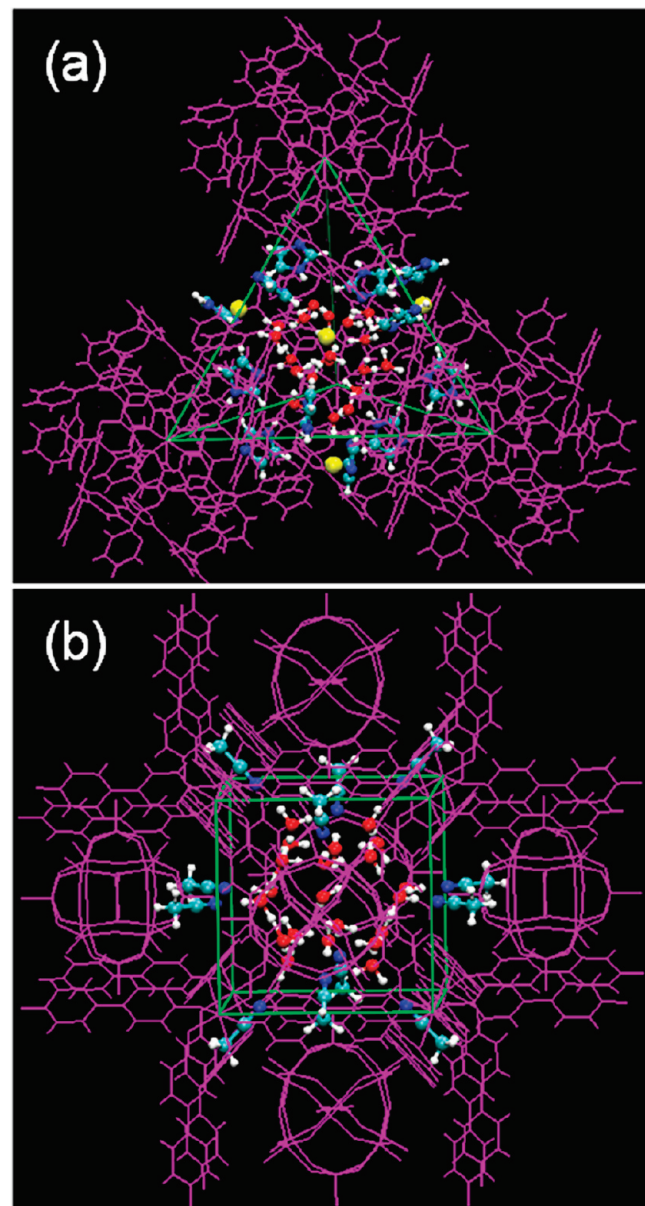


**Figure 1.** Schematic illustrations of the QM/MM calculated systems used in the work for (a) the  $(\text{H}_2\text{O})_{21}$  cluster confined in a tetrahedral host and (b) the  $\text{H}^+(\text{H}_2\text{O})_{21}$  cluster confined in a cubic host. The QM and MM regions are represented by the “ball and stick” and “wireframe” styles, respectively.

six neighboring  $[\text{PW}_{12}\text{O}_{40}]^{3-}$  clusters. For the QM/MM system, its total energy can be expressed as

$$E_{\text{tot}} = \left\langle \psi_{\text{QM}} | H_{\text{QM}} - \sum_i \sum_M \frac{Q_M}{r_{i,M}} | \psi_{\text{QM}} \right\rangle + \sum_{\alpha} \sum_M \frac{Z_{\alpha} Q_M}{R_{\alpha,M}} + 4 \sum_{\alpha} \sum_M \varepsilon_{\alpha,M} \left[ \left( \frac{\sigma_{\alpha,M}}{R_{\alpha,M}} \right)^{12} - \left( \frac{\sigma_{\alpha,M}}{R_{\alpha,M}} \right)^6 \right] + E_{\text{MM}} \quad (1)$$

where  $H_{\text{QM}}$  is the Hamiltonian of the QM region in a vacuum, and  $-\sum_i \sum_M (Q_M/r^{i,M})$  represents the electrostatic interactions between electrons (denoted by  $i$ ) of the QM region and the partial atomic charges on the atoms in the MM region

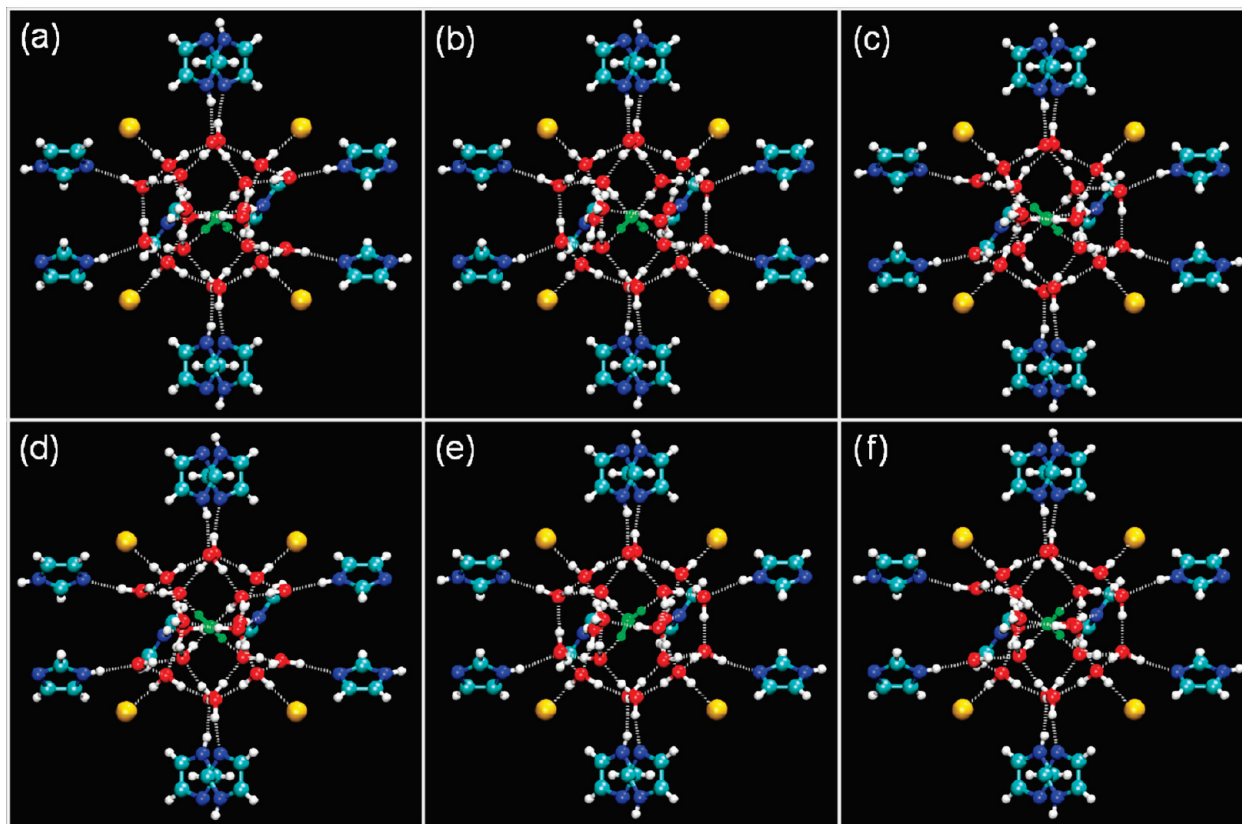


**Figure 2.** Illustrations of the six low-lying structures for the  $(\text{H}_2\text{O})_{21}$  cluster embedded with imidazole molecules and  $\text{Br}^-$  ions in the tetrahedral crystal host (Model 1). They are denoted as (a) the W1 structure; (b) the W2 structure; (c) the W3 structure; (d) the W4 structure; (e) the W5 structure; (f) the W6 structure. The interior water molecule is represented by the green spheres. To better show the  $(\text{H}_2\text{O})_{21}$  cluster, the host and two imidazole molecules (front view) are removed.

( $M$  denotes an atom with partial atomic charge  $Q_M$ ). The second and third terms in eq 1 represent the electrostatic interactions between nuclei of the QM region and the partial atomic charges on the atoms in the MM region, and the van der Waals interactions between the QM atoms and the MM atoms. The last term in eq 1,  $E_{\text{MM}}$ , is taken as the steric energy of the MM region. It should be mentioned that the wave function of the QM region,  $\psi_{\text{QM}}$ , depends on the coordinates of atoms in the QM region and the MM region, due to the electrostatic interaction between two regions. In our QM/MM calculations, the van der Waals interaction between the QM and MM regions is described with the parameters from the universal force field (UFF),<sup>31</sup> which is applicable to all elements in the periodic table. Since the original UFF does not include the electrostatic interaction between atoms, we have obtained partial atomic charges on all atoms in the MM region by performing ab initio calculations on some small model systems (the details are provided in the Supporting Information), as adopted by others.<sup>32–34</sup>

For the QM region, a mixed basis set is employed for QM calculations. The 6-311++G\*\* basis set is used for the neutral or protonated water cluster, and the 6-31G\*\* basis set is used for the remaining atoms. For the QM subsystem of Model 2, we perform conventional B3LYP calculations. But for the QM subsystem of Model 1, we employ the generalized energy-based fragmentation (GEBF) method proposed by our group<sup>35–39</sup> to perform approximate B3LYP calculations (the results are denoted as GEBF-B3LYP results), as conventional B3LYP calculations

are quite expensive for such QM region. Our previous work has demonstrated that the GEBF/density functional theory (DFT) results reproduce conventional DFT results very well for a wide range of systems with much less computational costs.<sup>22,35–39</sup> In this work, all of the conventional QM calculations are performed with the Gaussian 03 program,<sup>40</sup> and the GEBF calculations are carried out with the LSQC quantum chemistry package.<sup>41</sup>

**2.2. Searching of Low-Lying Structures.** Since the number of low-lying structures of  $(\text{H}_2\text{O})_{21}$  and  $\text{H}^+(\text{H}_2\text{O})_{21}$  confined in the crystal hosts is enormous, we have adopted the following strategy to determine a few low-lying structures for the two clusters.

First, the basin-hopping Monte Carlo (BHMC) optimization method<sup>42</sup> with a mixed empirical force field was used to produce a large number of low-lying structures for two model systems. For two crystal hosts, the van der Waals parameters are taken from the UFF, and the partial atomic charges are obtained as described above. The all-atom optimized potentials for liquid simulations (OPLS-AA) force field<sup>43</sup> is used for organic molecules and  $\text{Br}^-$  ions, and the four-site water (TIP4P) model<sup>44</sup> is used for the water molecules of neutral and protonated water clusters. For the hydronium ion in the protonated water cluster, the pyramidal model proposed by Kozak and Jordan<sup>45</sup> without the polarization effects is used, but their van der Waals parameters are also taken from the TIP4P model. During the BHMC simulation, each water molecule and hydronium in the water clusters is allowed to move freely, while all remaining atoms in

**Table 1.** Structural Characteristics ( $\text{\AA}$ ) and Relative Energies (kcal/mol) for the  $(\text{H}_2\text{O})_{21}$  Cluster Embedded with Imidazole Molecules and  $\text{Br}^-$  Ions in the Tetrahedral Crystal Host (Model 1), as well as Relative Energies of the  $(\text{H}_2\text{O})_{21}$  Cluster without the Crystal Host (Model 1a) and without Imidazole Molecules and  $\text{Br}^-$  Ions (Model 1b)

structure	rmsd	$N_{\text{HB}}$	$R_{\text{O}-\text{O}}$	$\Delta E^a$			$\Delta E_{\text{V}}^b$
				Model 1	Model 1a	Model 1b	
W1	0.18	32	2.705	0.00	0.00	0.00	57.03
W2	0.21	32	2.710	1.54	1.24	5.52	63.55
W3	0.22	32	2.705	2.01	1.06	6.00	63.20
W4	0.21	32	2.702	2.57	1.37	4.70	61.97
W5	0.17	32	2.713	3.45	2.50	3.56	60.85
W6	0.19	32	2.702	5.95	3.89	1.30	57.91

<sup>a</sup>  $\Delta E$  is the relative energy with respect to the W1 structure. <sup>b</sup>  $\Delta E_{\text{V}}$  is the relative energy of the  $(\text{H}_2\text{O})_{21}$  cluster in Model 1 with respect to the lowest-lying structure of the free  $(\text{H}_2\text{O})_{21}$  cluster in vacuum ( $-1605.999808$  au at the GEBF-B3LYP/6-311++G\*\* level<sup>22</sup>).

the surroundings (organic molecules, ions, and the crystal hosts) are fixed according to the experimental crystallographic data. The simulation was run for a total of  $2 \times 10^6$  steps to create a large database for low-lying structures (about 1500 local minima).

Next, for 300 lowest-energy local minima derived from the BHMC optimization process described above, we carry out single-point QM/MM calculations and rank these minimum structures in the increasing order. Then, the 30 structures with lowest QM/MM energies are used as the starting structures for further geometry optimization at the QM/MM level. During the geometry optimization, only the water clusters are flexible, and the other regions are fixed. Finally, to obtain more accurate energies, we perform single-point QM/MM calculations with a larger basis set (6-311++G\*\* basis set for all atoms in the QM region) at the corresponding optimized structures obtained with a mixed basis set.

### 3. RESULTS AND DISCUSSION

**3.1. Model 1.** On the basis of the QM/MM results, six low-lying structures (denoted as  $W_n$ ,  $n = 1-6$ ) of  $(\text{H}_2\text{O})_{21}$  confined in the tetrahedral host are displayed in Figure 2. All of these structures exist as a dodecahedral cage structure with one interior water molecule, which is quite consistent with the crystal structure observed experimentally.<sup>16</sup> Specifically, the root-mean-square distances (rmsd) between the oxygen skeletons of the crystal structure and those of six low-lying structures are found to be only about 0.2  $\text{\AA}$  (as shown in Table 1). These data suggest that our calculations reproduce the experimental structure quite well. On the other hand, it is also interesting to analyze the relevant H-bond network for these low-lying structures of  $(\text{H}_2\text{O})_{21}$ , which is difficult to be determined experimentally. Here the criterion for defining a H-bond is chosen to be the O–X ( $X = \text{O}$ ,  $\text{N}$ , and  $\text{Br}^-$ ) distance less than 3.5  $\text{\AA}$  and the O–H–X angle larger than  $150^\circ$ . It can be seen from Figure 2 that each of these structures has 16 extrinsic H-bonds with 12 imidazole molecules and 4  $\text{Br}^-$  ions, although these structures have different intrinsic H-bond topologies. Among 16 extrinsic H-bonds, 10 water molecules on the surface of the cage act as the H-bond donors to form 6 H-bonds ( $\text{O}-\text{H}\cdots\text{N}$ ) with 6

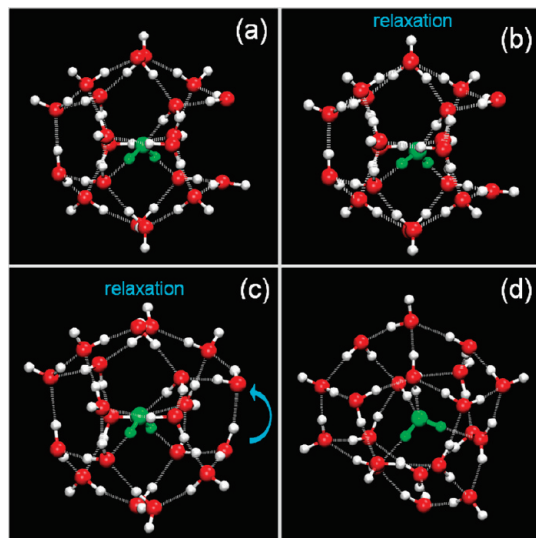


**Figure 3.** (a) The optimized W1 structures of the  $(\text{H}_2\text{O})_{21}$  cluster in (a) Model 1, (b) Model 1A (optimized Model 1a), and (c) Model 1B (optimized Model 1b). (d) The lowest-lying structure of the  $(\text{H}_2\text{O})_{21}$  cluster in vacuum from ref 22.

imidazole molecules and 4 H-bonds ( $\text{O}-\text{H}\cdots\text{Br}^-$ ) with 4  $\text{Br}^-$  ions, respectively. Another 6 water molecules on the surface serve as the H-bond acceptors to form 6 H-bonds ( $\text{O}\cdots\text{H}-\text{N}$ ) with other 6 imidazole molecules. The same number of extrinsic H-bonds for all six low-lying structures means that the structures of  $(\text{H}_2\text{O})_{21}$  cluster confined in the crystal host seem to be highly selective, which is probably induced by 12 imidazole molecules and 4  $\text{Br}^-$  ions in the crystal host. We have investigated the H-bond strengths in dimers of water– $\text{Br}^-$ , water–imidazole, and water–water. As shown in Figure S3 of the Supporting Information, the calculated binding energies suggest that the H-bonds in water– $\text{Br}^-$  and water–imidazole are significantly stronger than that in the water dimer. Hence, the water molecules on the cluster surface prefer to form the extrinsic H-bonds with imidazole molecules and  $\text{Br}^-$  ions.

Recently, our calculations<sup>22</sup> have revealed that the lowest-energy structure of the  $(\text{H}_2\text{O})_{21}$  cluster in vacuum is a one-centered dodecahedral cage (see Figure 3d), which is structurally similar to all six low-lying structures described above. Hence, the main structural feature of the  $(\text{H}_2\text{O})_{21}$  cluster is captured by the confined  $(\text{H}_2\text{O})_{21}$  cluster in Model 1. However, a close examination shows that there are 34 intrinsic H-bonds in the free  $(\text{H}_2\text{O})_{21}$  cluster but only 32 intrinsic H-bonds in the confined  $(\text{H}_2\text{O})_{21}$  clusters. In addition, the average O–O distance in the confined clusters is in the range from 2.702 to 2.713  $\text{\AA}$ , somewhat shorter than 2.783  $\text{\AA}$  in the free  $(\text{H}_2\text{O})_{21}$  cluster. These results suggest that the  $(\text{H}_2\text{O})_{21}$  cluster in the crystal host is slightly compressed by the surroundings around it. Our single-point QM/MM calculations show that the confined structures of  $(\text{H}_2\text{O})_{21}$  are much higher in energy than the lowest-energy structure of the free  $(\text{H}_2\text{O})_{21}$  cluster in vacuum by more than 57.0 kcal/mol, as shown in Table 1.

It is interesting to know how the local surroundings affect the relative energies of various  $(\text{H}_2\text{O})_{21}$  structures. To investigate the influence of the crystal host and small molecules (or ions) around the  $(\text{H}_2\text{O})_{21}$  cluster, we define two models from Model 1. Model 1a is obtained by removing the crystal host from Model 1,

**Table 2. Structural Characteristics (Å) and Relative Energies ( $\Delta E$ , kcal/mol) for the  $(\text{H}_2\text{O})_{21}$  Cluster in Model 1A (Optimized Model 1a) and Model 1B (Optimized Model 1b). Here the Relative Energies Are Relative to the Corresponding Structure of the  $(\text{H}_2\text{O})_{21}$  Cluster in Model 1**

structure	Model 1A			Model 1B		
	$N_{\text{HB}}$	$R_{\text{O}-\text{O}}$	$\Delta E$	$N_{\text{HB}}$	$R_{\text{O}-\text{O}}$	$\Delta E$
W1	32	2.710	-7.27	33	2.800	-35.18
W2	32	2.712	-6.78	32	2.820	-33.52
W3	32	2.710	-8.88	33	2.823	-38.17
W4	32	2.704	-9.24	32	2.819	-32.33
W5	32	2.713	-7.96	32	2.797	-28.66
W6	32	2.700	-6.6	33	2.816	-33.52

and Model 1b is derived by removing all imidazole molecules and  $\text{Br}^-$  ions (but the crystal host is kept) from Model 1. As shown in Table 1, the relative energy order for various isomers of Model 1a agrees reasonably well with the original order of Model 1, except that the relative energy of W2 and W3 is inverted. However, a very different relative order is observed for Model 1b, compared to the results of Model 1.

To further shed insight into how the local surroundings influences the structures of the  $(\text{H}_2\text{O})_{21}$  cluster, we have optimized the structures of six isomers of Model 1a and Model 1b with the GEBF-B3LYP method. The optimized Model 1a or Model 1b is defined as Model 1A or Model 1B for simplicity. As shown in Figure 3 parts a and b, in the corresponding W1 isomer of both models (Model 1 and Model 1A), the H-bond networks (32 intrinsic and 16 extrinsic H-bonds) and the average O–O distance in the  $(\text{H}_2\text{O})_{21}$  cluster are very similar. From Table 2, one can see that the isomers of Model 1A are always more stable than those of Model 1 (as expected), but by less than 10.0 kcal/mol. This result demonstrates that the crystal host has a small influence on the structures of the  $(\text{H}_2\text{O})_{21}$  cluster, and its main role is to act as a container to accommodate small molecules and ions. However, in the corresponding W1 isomer of Model 1B (Figure 3c), one can see that two surface water molecules on the right-hand side form a new intrinsic H-bond. Furthermore, the average O–O distance in the W1 isomer increases from 2.705 (Model 1) to 2.800 Å (Model 1B), showing a significant expansion of the oxygen framework. On the other hand, one can see from Table 2 that the isomers of the confined  $(\text{H}_2\text{O})_{21}$  cluster in Model 1B are much lower in energy (by more than 30.0 kcal/mol) than the corresponding isomers in Model 1. Therefore, one can conclude that imidazole molecules and  $\text{Br}^-$  ions in the crystal host play an essential role in tuning the structures of the  $(\text{H}_2\text{O})_{21}$  cluster.

**3.2. Model 2.** In this model, the  $\text{H}^+(\text{H}_2\text{O})_{21}$  cluster and acetonitrile molecules are confined in the cubic MOF cavity with six  $[\text{PW}_{12}\text{O}_{40}]^{3-}$  anions in neighboring environments. This model is assumed to be reasonable for studying the effect of the local environments on the  $\text{H}^+(\text{H}_2\text{O})_{21}$  cluster. For convenience, the host is denoted as the combination of the cubic MOF cavity and six  $[\text{PW}_{12}\text{O}_{40}]^{3-}$  anions. The six low-lying structures (denoted as PW $n$ ,  $n = 1-6$ ) of Model 2 are shown in Figure 4. It can be seen that 12 surface water molecules form 12 H-bonds ( $\text{O}-\text{H} \cdots \text{N}$ ) with 12 acetonitrile molecules so that the cluster has a common hexahedral  $(\text{H}_2\text{O})_{20}$  shell, which is similar to the experimental X-ray structure.<sup>17</sup> Note that the H-bond strength in

the water–acetonitrile dimer is nearly identical to that in the water dimer (see Figure S3 of the Supporting Information). The fact that the surface water molecules tend to form extrinsic H-bonds with acetonitrile molecules indicates that the cooperative many-body effects may lead to stronger water–acetonitrile H-bonds than water–water H-bonds. For example, in the PW1 structure, the average N–O distance for water–acetonitrile H-bonds is 2.872 Å, being 0.175 Å shorter than that in the water–acetonitrile dimer, while the average O–O distance for water–water H-bonds is 2.754 Å, being 0.159 Å shorter than that in the water dimer.

Experimentally, the X-ray diffraction measurements<sup>17</sup> show that the additional water molecule (or the  $\text{H}_3\text{O}^+$  ion) is located in the center of the hexahedral  $(\text{H}_2\text{O})_{20}$  shell. However, our calculations show that the location of the additional  $\text{H}_2\text{O}$  (or the  $\text{H}_3\text{O}^+$  ion) is not unique in six low-lying structures. For example, the additional water molecule (or the  $\text{H}_3\text{O}^+$  ion) lies on the surface of the PW2 structure but in the center of the PW6 structure. Apparently, the confined structures with vacant cage will be very unstable in the gas phase. As shown in Table 3, the energies of such structures in vacuum are higher than the lowest-lying structure of the free  $\text{H}^+(\text{H}_2\text{O})_{21}$  cluster by around 50.0 kcal/mol. Hence, the vacant cage structures are stabilized by the H-bond interactions between the protonated water cluster and the acetonitrile molecules embedded in the crystal host. In six low-lying structures shown in Figure 4, the proton always exists in the Eigen  $\text{H}_3\text{O}^+$  form rather than the Zundel  $\text{H}_5\text{O}_2^+$  form, and it tends to locate on the surface of the cluster (except in the PW4 structure). The  $\text{H}_3\text{O}^+$  ion is stabilized by three H-bonds with three water molecules in the structures W1, W2, W4, and W5, but with two water molecules and one acetonitrile molecule in the W3 and W6 structures. Among the six structures, the oxygen skeleton of the PW6 structure is closest to the X-ray structure with the rmsd of 0.33 Å.<sup>17</sup> The relatively large deviation between the calculated and X-ray structures for the confined  $\text{H}^+(\text{H}_2\text{O})_{21}$  cluster may be attributed to the fact that the  $\text{H}^+(\text{H}_2\text{O})_{21}$  cluster has an inherently flexible structure due to the presence of excess proton and the temperature effect is not considered in our calculations.

Recent ab initio calculations<sup>27</sup> showed that the lowest-energy structure of the free  $\text{H}^+(\text{H}_2\text{O})_{21}$  cluster is a dodecahedral  $(\text{H}_2\text{O})_{20}$  cage containing an interior water molecule, with the proton on the cluster surface in the Eigen  $\text{H}_3\text{O}^+$  form, as shown in Figure 5d. Furthermore, there are 34 H-bonds in the free  $\text{H}^+(\text{H}_2\text{O})_{21}$  cluster, but only 24 to 27 H-bonds in the  $\text{H}^+(\text{H}_2\text{O})_{21}$  motif of six low-lying structures of Model 2. Thus, the structural feature of the free  $\text{H}^+(\text{H}_2\text{O})_{21}$  cluster is quite different from that of the confined  $\text{H}^+(\text{H}_2\text{O})_{21}$  cluster (the latter tends to have a hexahedral cage and much less H-bonds).

Similar to the Model 1 case, we also define two simplified models from Model 2 to analyze the influence of the local surroundings on the energies and structures of the  $\text{H}^+(\text{H}_2\text{O})_{21}$  cluster. Model 2a and Model 2b are obtained by removing the host and the acetonitrile molecules from Model 2, respectively. Accordingly, the optimized Model 2a (or Model 2b) is denoted as Model 2A (or Model 2B). As shown in Table 3, we can find that the relative energy order in both Model 2a and Model 2b are distinct from the original energy order in Model 2. As shown in Figure 5, in the corresponding PW1 structure of Model 2A, five new intrinsic H-bonds are formed, compared to that of Model 2. In the meanwhile, the average O–O distance is slightly increased

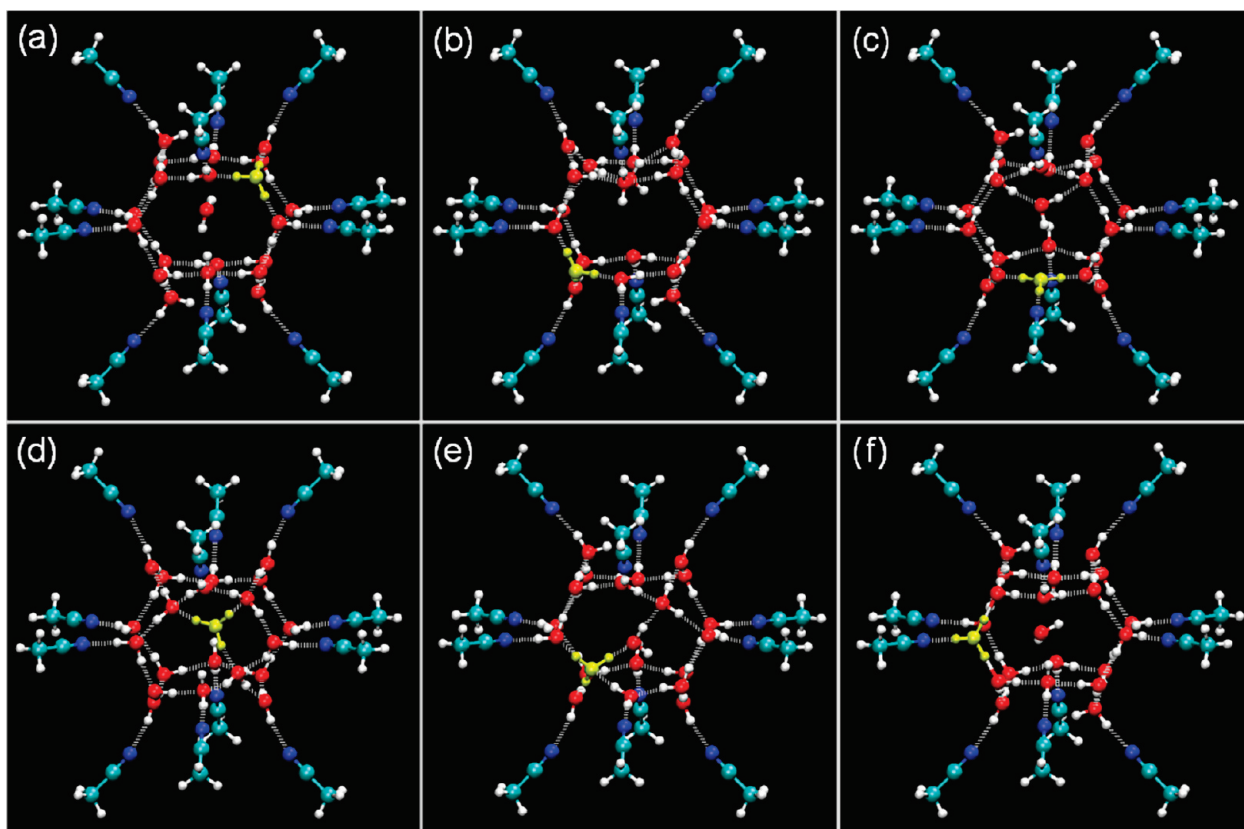


**Figure 4.** Illustrations of the six low-lying structures for the  $\text{H}^+(\text{H}_2\text{O})_{21}$  cluster embedded with acetonitrile molecules in the cubic crystal host (Model 2). They are denoted as (a) the PW1 structure; (b) the PW2 structure; (c) the PW3 structure; (d) the PW4 structure; (e) the PW5 structure; (f) the PW6 structure. The Eigen  $\text{H}_3\text{O}^+$  cation is represented by the yellow spheres.

**Table 3. Structural Characteristics (Å) and Relative Energies (kcal/mol) for the  $\text{H}^+(\text{H}_2\text{O})_{21}$  Cluster Embedded with Acetonitrile Molecules in the Cubic Crystal Host (Model 2), as well as Relative Energies of the  $\text{H}^+(\text{H}_2\text{O})_{21}$  Cluster without the Crystal Host (Model 2a) and without Acetonitrile Molecules (Model 2b)**

structure	rmsd	$N_{\text{HB}}$	$R_{\text{O}-\text{O}}$	$\Delta E^a$			$\Delta E_V^b$
				Model 2	Model 2a	Model 2b	
PW1	0.53	24	2.754	0.00	0.00	0.00	53.89
PW2	0.53	26	2.750	1.36	-3.66	-0.24	48.42
PW3	0.48	26	2.749	2.07	-5.95	1.27	47.05
PW4	0.60	27	2.728	3.92	-4.60	-0.22	44.75
PW5	0.50	26	2.746	5.45	-3.75	4.44	49.46
PW6	0.33	24	2.777	6.72	0.12	7.82	50.35

<sup>a</sup>  $\Delta E$  is the relative energy with respect to the PW1 structure. <sup>b</sup>  $\Delta E_V$  is the relative energy of the  $\text{H}^+(\text{H}_2\text{O})_{21}$  cluster in Model 2 with respect to the lowest-lying structure of the free  $\text{H}^+(\text{H}_2\text{O})_{21}$  cluster in vacuum ( $-1606.390435$  au at the B3LYP/6-311++G\*\* level of theory<sup>27</sup>).

from 2.754 (model 2) to 2.786 Å (Model 2A). The PW1 structure of the confined  $\text{H}^+(\text{H}_2\text{O})_{21}$  cluster in Model 2A is 27.5 kcal/mol lower in energy than the corresponding structure in Model 2, as shown in Table 4. Similar phenomena can also be observed, when the structures and energies of Model 2B are compared with those of Model 2. These results suggest that the structures and energies of the confined  $\text{H}^+(\text{H}_2\text{O})_{21}$  cluster are significantly modulated by not only acetonitrile molecules but

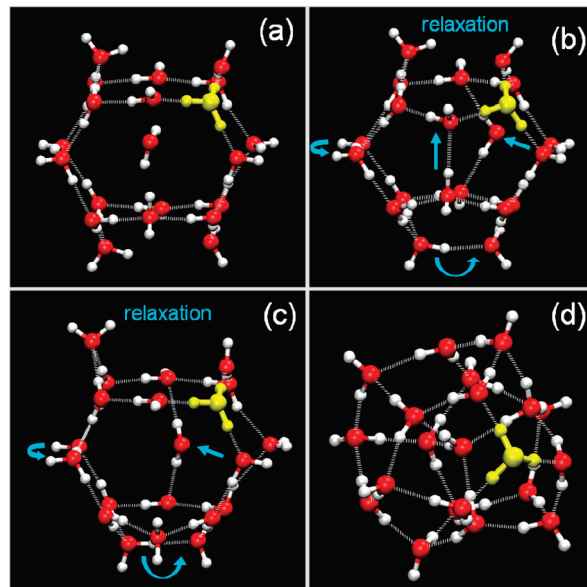


**Figure 5.** (a) The optimized PW1 structures of the  $\text{H}^+(\text{H}_2\text{O})_{21}$  cluster in (a) Model 2, (b) Model 2A (optimized Model 2a), and (c) Model 2B (optimized Model 2b). (d) The lowest-energy structure of the  $\text{H}^+(\text{H}_2\text{O})_{21}$  cluster in vacuum from ref 27.

also the crystal host. The significant influence of the host on the  $\text{H}^+(\text{H}_2\text{O})_{21}$  cluster can be attributed to the fact that the

**Table 4. Structural Characteristics (Å) and Relative Energies ( $\Delta E$ , kcal/mol) for the  $\text{H}^+(\text{H}_2\text{O})_{21}$  Cluster in Model 2A (Optimized Model 2a) and Model 2B (Optimized Model 2b). Here the Relative Energies Are Relative to the Corresponding Structure of the  $\text{H}^+(\text{H}_2\text{O})_{21}$  Cluster in Model 2**

structure	Model 2A			Model 2B		
	$N_{\text{HB}}$	$R_{\text{O}-\text{O}}$	$\Delta E$	$N_{\text{HB}}$	$R_{\text{O}-\text{O}}$	$\Delta E$
PW1	29	2.786	-27.51	28	2.811	-15.28
PW2	30	2.776	-29.81	27	2.803	-7.96
PW3	27	2.749	-9.57	27	2.802	-11.18
PW4	28	2.747	-10.2	28	2.790	-10.86
PW5	26	2.737	-3.58	30	2.780	-25.03
PW6	30	2.791	-33.54	29	2.804	-24.22

$\text{H}^+(\text{H}_2\text{O})_{21}$  cluster is strongly polarized by the external electrostatic field of the host (mainly from six  $[\text{PW}_{12}\text{O}_{40}]^{3-}$  anions).

## 4. CONCLUSIONS

The structural features of the magic number  $(\text{H}_2\text{O})_{21}$  and  $\text{H}^+(\text{H}_2\text{O})_{21}$  clusters confined in the crystal hosts have been investigated by using the hybrid QM/MM method. For the neutral  $(\text{H}_2\text{O})_{21}$  cluster in the tetrahedral host, its low-lying structures are found to exist as a dodecahedral cage with one interior water molecule, forming 16 extrinsic H-bonds ( $\text{O}-\text{H}\cdots\text{N}$  or  $\text{Br}^-$ ) with imidazole molecules and  $\text{Br}^-$  ions. Furthermore, the calculated oxygen skeletons of this cluster are in good accord with the corresponding X-ray data. The confined  $(\text{H}_2\text{O})_{21}$  cluster possesses the main structural features of the lowest-energy structure of the free  $(\text{H}_2\text{O})_{21}$  cluster, although it has slightly less intrinsic H-bonds due to the competition of 12 imidazole molecules and 4  $\text{Br}^-$  ions as H-bond donors or acceptors. For the protonated  $\text{H}^+(\text{H}_2\text{O})_{21}$  cluster confined in the cubic MOF cavity, our calculations showed that its low-lying structures have a common hexahedral  $(\text{H}_2\text{O})_{20}$  shell, in which water molecules on the surface form 12 extrinsic H-bonds with acetonitrile molecules. For these low-lying structures, their overall shape is consistent with the experimental X-ray structure, but the additional  $\text{H}_2\text{O}$  (or the  $\text{H}_3\text{O}^+$  ion) may lie in the center of the cage or on the surface, while in the corresponding X-ray structure the  $\text{H}_3\text{O}^+$  ion is situated at the center of the cage. In addition, the proton in the confined  $\text{H}^+(\text{H}_2\text{O})_{21}$  cluster is found to exist in the Eigen  $\text{H}_3\text{O}^+$  form on the cluster surface. In comparison with the  $\text{H}^+(\text{H}_2\text{O})_{21}$  cluster in the gas phase, the confined  $\text{H}^+(\text{H}_2\text{O})_{21}$  cluster is significantly different in two aspects. One is that the confined  $\text{H}^+(\text{H}_2\text{O})_{21}$  cluster displays a hexahedral  $(\text{H}_2\text{O})_{20}$  cage, while the free one exists as a dodecahedral  $(\text{H}_2\text{O})_{20}$  cage. The other is that the confined cluster has much fewer intrinsic H-bonds than the free cluster, because of the need to form extrinsic H-bonds with acetonitrile molecules. On the other hand, we found that the MOF host plays an important role in tuning the structure of the  $\text{H}^+(\text{H}_2\text{O})_{21}$  cluster, which is in contrast to the negligible influence of the host on the structure of the  $(\text{H}_2\text{O})_{21}$  cluster. This fact may be attributed to the fact that the protonated water clusters are much more easily polarized by the external electrostatic field of the crystal host than the neutral water clusters. Our calculations are a great help for experimental scientists to understand the structures of neutral and protonated water clusters confined in the crystal hosts.

## ■ ASSOCIATED CONTENT

**S Supporting Information.** The details of the van der Waals parameters and partial atomic charges for atoms in the MM region, as well as the binding energies between water– $\text{Br}^-$ , water–imidazole, water–acetonitrile, and water–water dimers. This material is available free of charge via the Internet at <http://pubs.acs.org>.

## ■ AUTHOR INFORMATION

### Corresponding Author

\*E-mail: shuhua@nju.edu.cn.

## ■ ACKNOWLEDGMENT

This work was supported by the National Natural Science Foundation of China (Grants 21073086 and 20833003), the National Basic Research Program (Grant 2011CB808501), and China Postdoctoral Science Foundation (Grant No. 20100481111).

## ■ REFERENCES

- Buck, U.; Huisken, F. *Chem. Rev.* **2000**, *100*, 3863–3890.
- Ludwig, R. *Angew. Chem., Int. Ed.* **2001**, *40*, 1808–1827.
- Hartke, B. *Angew. Chem., Int. Ed.* **2002**, *41*, 1468–1487.
- Keutsch, F. N.; Cruzan, J. D.; Saykally, R. J. *Chem. Rev.* **2003**, *103*, 2533–2577.
- Chang, H.-C.; Wu, C.-C.; Kuo, J.-L. *Int. Rev. Phys. Chem.* **2005**, *24*, 553–578.
- Nauta, K.; Miller, R. E. *Science* **2000**, *287*, 293–295.
- Miyazaki, M.; Fujii, A.; Ebata, T.; Mikami, N. *Science* **2004**, *304*, 1134–1137.
- Rodriguez-Cuamatzi, P.; Vargas-Diaz, G.; Hopfl, H. *Angew. Chem., Int. Ed.* **2004**, *43*, 3041–3044.
- Shin, J.-W.; Hammer, N. I.; Diken, E. G.; Johnson, M. A.; Walters, R. S.; Jaeger, T. D.; Duncan, M. A.; Christie, R. A.; Jordan, K. D. *Science* **2004**, *304*, 1137–1141.
- Ghosh, S. K.; Bharadwaj, P. K. *Angew. Chem., Int. Ed.* **2004**, *43*, 3577–3580.
- Ghosh, S. K.; Ribas, J.; Fallah, M. S. E.; Bharadwaj, P. K. *Inorg. Chem.* **2005**, *44*, 3856–3862.
- Dai, F. N.; He, H. Y.; Sun, D. F. *J. Am. Chem. Soc.* **2008**, *130*, 14604–14605.
- Yoshizawa, M.; Kusukawa, T.; Kawano, M.; Ohhara, T.; Tanaka, I.; Kurihara, K.; Niimura, N.; Fujita, M. *J. Am. Chem. Soc.* **2005**, *127*, 2798–2799.
- Ou, Y.-C.; Lin, Z.-J.; Tong, M.-L. *CrystEngComm* **2010**, *12*, 4020–4023.
- Zuhayra, M.; Kampen, W. U.; Henze, E.; Soti, Z.; Zsolnai, L.; Huttner, G.; Oberdorfer, F. A. *J. Am. Chem. Soc.* **2006**, *128*, 424–425.
- Cao, M.-L.; Wu, J.-J.; Mo, H.-J.; Ye, B.-H. *J. Am. Chem. Soc.* **2009**, *131*, 3458–3459.
- Duan, C. Y.; Wei, M. L.; Guo, D.; He, C.; Meng, Q. *J. J. Am. Chem. Soc.* **2010**, *132*, 3321–3330.
- Wei, M. L.; He, C.; Hua, W.; Duan, C. Y.; Li, S.; Meng, Q. *J. J. Am. Chem. Soc.* **2006**, *128*, 13318–13319.
- Hodges, M. P.; Wales, D. J. *J. Chem. Phys. Lett.* **2000**, *324*, 279–288.
- James, T.; Wales, D. J.; Hernandez-Rojas, J. *J. Chem. Phys. Lett.* **2005**, *415*, 302–307.
- Hartke, B. *Phys. Chem. Chem. Phys.* **2003**, *5*, 275–284.
- Yang, Z.; Hua, S.; Hua, W.; Li, S. *J. Phys. Chem. A* **2010**, *114*, 9253–9261.
- Searcy, J. Q.; Fenn, J. B. *J. Chem. Phys.* **1974**, *61*, 5282–5288.
- James, T.; Wales, D. J. *J. Chem. Phys.* **2005**, *122*, 134306.
- Kuo, J.-L.; Klein, M. L. *J. Chem. Phys.* **2005**, *122*, 024516.

- (26) Wu, C.-C.; Lin, C.-K.; Chang, H.-C.; Jiang, J.-C.; Kuo, J.-L.; Klein, M. L. *J. Chem. Phys.* **2005**, *122*, 074315.
- (27) Kus, T.; Lotrich, V. F.; Perera, A.; Bartlett, R. J. *J. Chem. Phys.* **2009**, *131*, 104313.
- (28) Choi, T. H.; Jordan, K. D. *J. Phys. Chem. B* **2010**, *114*, 6932–6936.
- (29) Lee, S.-W.; Freivogel, P.; Schindler, T.; Beauchamp, J. L. *J. Am. Chem. Soc.* **1998**, *120*, 11758–11765.
- (30) Singh, N. J.; Park, M.; Min, S. K.; Suh, S. B.; Kim, K. S. *Angew. Chem., Int. Ed.* **2006**, *45*, 3795–3800.
- (31) Rappe, A. K.; Casewit, C. J.; Colwell, K. S.; Goddard, W. A., III; Skiff, W. M. *J. Am. Chem. Soc.* **1992**, *114*, 10024–10035.
- (32) Babarao, R.; Jiang, J. W. *J. Am. Chem. Soc.* **2009**, *131*, 11417–11425.
- (33) Farha, O. K.; Yazaydin, A. O.; Eryazici, I.; Malliakas, C. D.; Hauser, B. G.; Kanatzidis, M. G.; Nguyen, S. T.; Snurr, R. Q.; Hupp, J. T. *Nature Chem.* **2010**, *2*, 944–948.
- (34) Vaidhyanathan, R.; Iremonger, S. S.; Shimizu, G. K. H.; Boyd, P. G.; Alavi, S.; Woo, T. K. *Science* **2010**, *330*, 650–653.
- (35) Li, W.; Li, S.; Jiang, Y. *J. Phys. Chem. A* **2007**, *111*, 2193–2199.
- (36) Li, S.; Li, W. *Annu. Rep. Prog. Chem., Sect. C: Phys. Chem.* **2008**, *104*, 256–271.
- (37) Hua, W.; Fang, T.; Li, W.; Yu, J.-G.; Li, S. *J. Phys. Chem. A* **2008**, *112*, 10864–10872.
- (38) Li, W.; Dong, H.; Li, S. *Progress in Theoretical Chemistry and Physics*; Springer-Verlag: Berlin, 2008; Vol. 18, pp 289–299.
- (39) Hua, S.; Hua, W.; Li, S. *J. Phys. Chem. A* **2010**, *114*, 8126–8134.
- (40) Frisch, M. J.; Trucks, G. W.; Schlegel, H. B.; Scuseria, G. E.; Robb, M. A.; Cheeseman, J. R.; Montgomery, J. A., Jr.; Vreven, T.; Kudin, K. N.; Burant, J. C.; Millam, J. M.; Iyengar, S. S.; Tomasi, J.; Barone, V.; Mennucci, B.; Cossi, M.; Scalmani, G.; Rega, N.; Petersson, G. A.; Nakatsuji, H.; Hada, M.; Ehara, M.; Toyota, K.; Fukuda, R.; Hasegawa, J.; Ishida, M.; Nakajima, T.; Honda, Y.; Kitao, O.; Nakai, H.; Klene, M.; Li, X.; Knox, J. E.; Hratchian, H. P.; Cross, J. B.; Adamo, C.; Jaramillo, J.; Gomperts, R.; Stratmann, R. E.; Yazyev, O.; Austin, A. J.; Cammi, R.; Pomelli, C.; Ochterski, J. W.; Ayala, P. Y.; Morokuma, K.; Voth, G. A.; Salvador, P.; Dannenberg, J. J.; Zakrzewski, V. G.; Dapprich, S.; Daniels, A. D.; Strain, M. C.; Farkas, O.; Malick, D. K.; Rabuck, A. D.; Raghavachari, K.; Foresman, J. B.; Ortiz, J. V.; Cui, Q.; Baboul, A. G.; Clifford, S.; Cioslowski, J.; Stefanov, B. B.; Liu, G.; Liashenko, A.; Piskorz, P.; Komaromi, I.; Martin, R. L.; Fox, D. J.; Keith, T.; Al-Laham, M. A.; Peng, C. Y.; Nanayakkara, A.; Challacombe, M.; Gill, P. M. W.; Johnson, B.; Chen, W.; Wong, M. W.; Gonzalez, C.; Pople, J. A. *Gaussian 03*, revision D.01; Gaussian, Inc.: Wallingford, CT, 2004.
- (41) Li, S.; Li, W.; Fang, T.; Ma, J.; Hua, W.; Hua, S.; Jiang, Y. *Low-Scaling Quantum Chemistry (LSQC)*, version 2.0; Nanjing University: Nanjing, 2010.
- (42) Wales, D. J.; Doye, J. P. K. *J. Phys. Chem. A* **1997**, *101*, 5111–5116.
- (43) Jorgensen, W. L.; Maxwell, D. S.; Tirado-Rives, J. *J. Am. Chem. Soc.* **1996**, *118*, 11225–11236.
- (44) Jorgensen, W. L.; Chandrasekhar, J.; Madura, J. D.; Impey, R. W.; Klein, M. L. *J. Chem. Phys.* **1983**, *79*, 926–935.
- (45) Kozack, R. E.; Jordan, P. C. *J. Chem. Phys.* **1992**, *96*, 3131–3136.